A Simple Shear Test to Evaluate Material Ductility based on Specimens cut from Thin-Walled sections

Tore Tryland[1], Torodd Berstad[2]

[1]Benteler Aluminium Systems, Raufoss, Norway

[2]Department of Structural Engineering, Norwegian University of Science and Technology, Trondheim, Norway

1 Background

Both material variants shown in the crushing tests in figure 1 were aged to achieve the same yield stress like 280 MPa. In addition, some cutting angles were introduced to the upper end of the extruded profile to overcome the effect from geometrical uncertainties [1]. But, the results show some deviations from a well defined folding mode. The first variant shows two peaks to initiate folding and average force level about 190 kN, while the second test gave one peak and average force level about 220 kN. It is likely that this is the result from different strain hardening and anisotropy. It is also interesting to observe the locations with severe deformations whereas only some of them show fracture.

Fig. 1: Crushing tests with material variants that have the same yield stress

A shear test specimen with outer dimensions 80x150 mm has been used for several years to evaluate the ductility of materials cut from thin-walled sections [2], see figure 2. Note that the geometry to machine is complex, and this specimen is relatively large compared with the region that is severely deformed. Smaller test specimens that could be cut out transverse and 45º relative to aluminium extrusions has also been investigated [3], but then it may be more difficult to achieve acceptable accuracy. Therefore, the objective of this study was to investigate the possibilities and the accuracy that can be obtained by using a specimen holder that fits inside our uniaxial tensile test machine and a simple test specimen that has limited size outside the critical shear region.

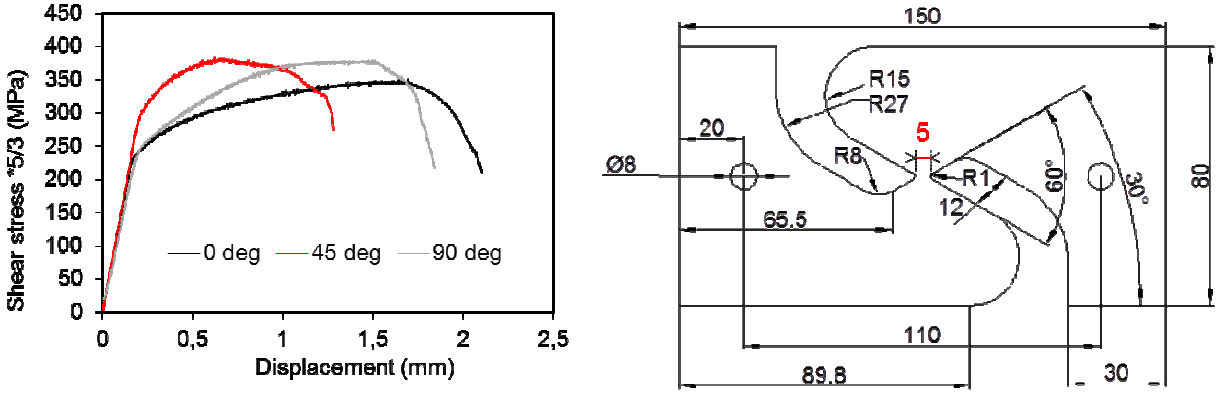

Fig. 2: Shear test results (adjusted with factor 5/3) as well as specimen geometry from Achani [2]

2 Specimen geometry and test procedure

The test specimen is cut out from thin-walled sections, and eventual recrystallized layers are therefore included at the two opposite surfaces with no machining. The overall specimen geometry is reduced to 12x60 mm, while the critical region is kept with 5 mm width in between the two grooves that are machined with radius 1 mm. The specimen geometry is defined in figure 3, while the holder and test arrangement are shown in figure 4.

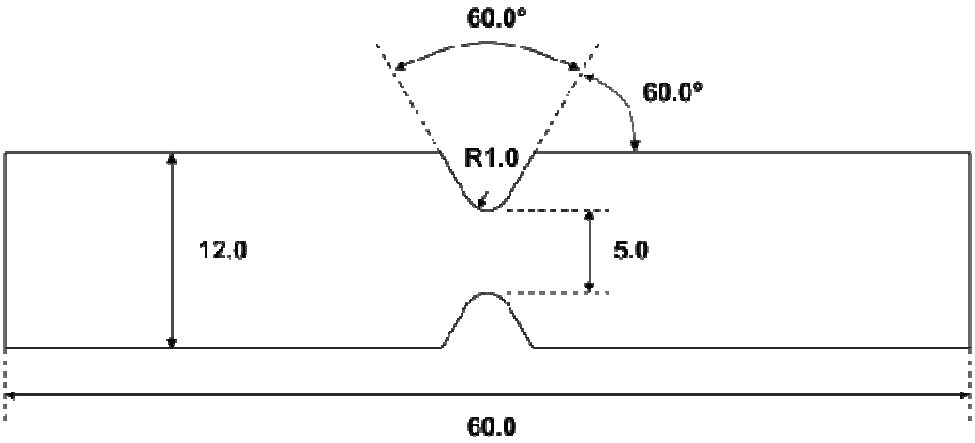

Fig. 3: Simplified test specimen geometry

The specimen holder was designed to fit inside our testing machine with round “bars” to meet the automatic extensometer mounting as used for uniaxial tensile tests. Note that many parallel tests are planned to evaluate the local variation in material properties, and it is therefore important that the test arrangement works well with an industrial test procedure. The technicians that operate the machine were therefore involved to test out the mounting of the specimen inside the holder as well as the positioning of the test specimen inside the testing machine. Herein it is important to notice the test arrangement with holder and fixation brackets has weight like 870 gram, and some care has to be taken when handling these parts to avoid damage of the critical cross-section with dimension 5 mm times the thickness of the test specimen. Therefore, it may be an idea to place the specimen inside the holder when the holder is still inside the testing machine, and fix the specimen by the brackets and a careful torque of the cylinder head bolts. The specimen corners require support inside the holder, and there has to be some gap between the upper and the lower part of the holder. But the exact gap between these two parts seems not important. The distance between the two circular bars that fix the holder inside the testing machine is somewhat above 110 mm, and one millimetre reduced gap results in about 0.5º rotation of the test specimen.

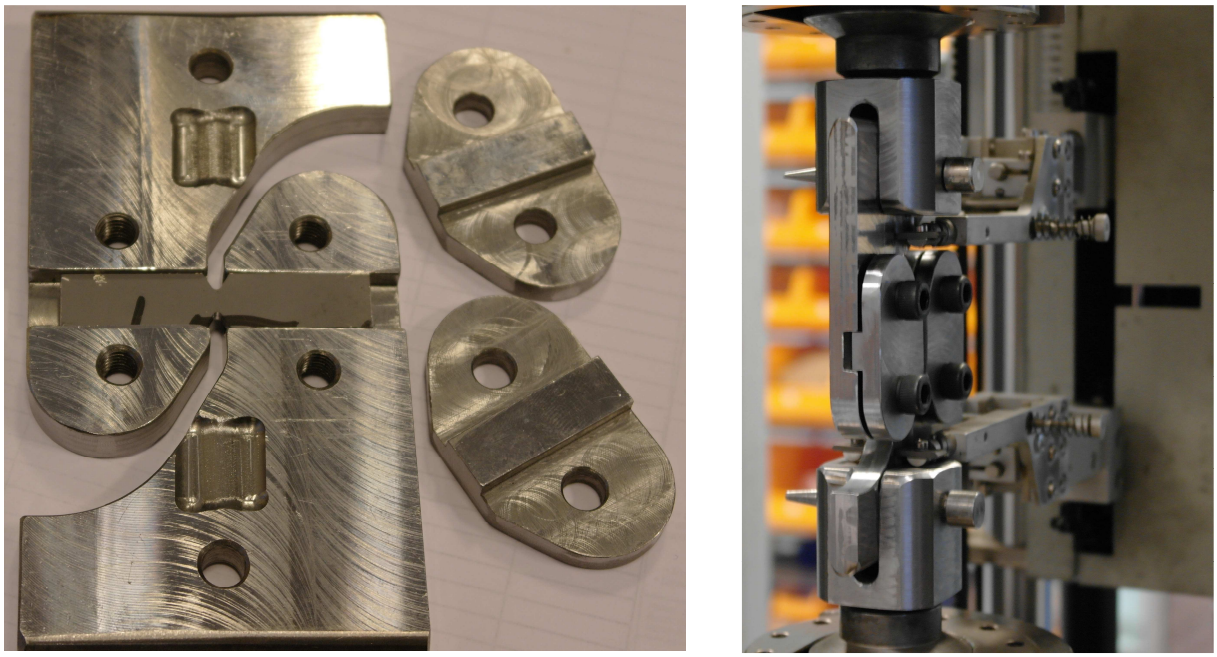

Fig. 4: Test specimen, holder and fixation brackets as well as test arrangement with extensometers

2.1 Initial tests to evaluate some possibilities with the proposed test specimen

Some initial tests were run to evaluate whether the proposed shear test was able to distinguish between two material variants that show the same results in a uniaxial tensile test. The response curves shown in figure 5 follow each other into some level of plastic deformation, and the results indicate ± 8 MPa as variation in strength. Herein it is important to notice that the nominal stress at the ordinate is scaled by the factor 5/3 to reach a similar strength level in these shear test as we are used to see from a uniaxial tensile test. Moreover, the tests were run with 70 mm extensometers length, and the first results show significant variation after about 1.3 mm displacement.

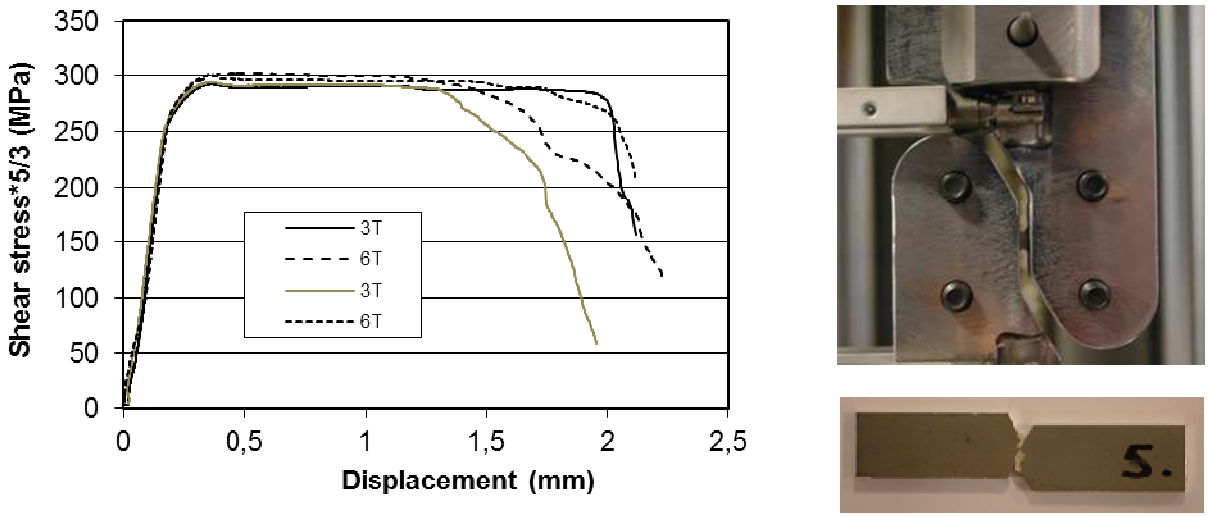

Fig. 5: Results from the initial four tests, test arrangement as well as one tested sample

The simple test specimen can also be stretched in the testing machine, and the results from two material variants that have the same results from a uniaxial tensile test are shown in figure 6. Herein, the two grooves with the small radius 1 mm result in relatively localised deformation well inside the extensometer length 10 mm. The observed behaviour is therefore similar to a plane strain tension test.

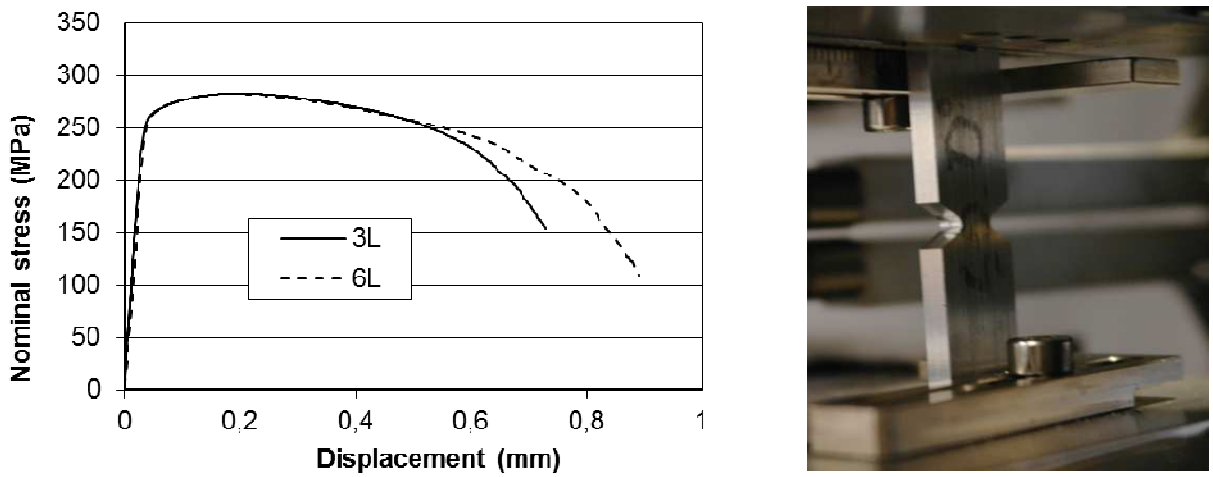

Fig. 6: Results from the initial two tests with stretching of the proposed test specimen

Both shear and stretch loading of the proposed test specimen indicates that the variant denoted (6) is more ductile than the variant denoted (3). Remember that both variants show the same results in a uniaxial tensile test, but the specimen geometry used herein results in a relatively narrow shear band and a localised region in tension. The specimen tears off when the plastic capacity that remains in it is equal to the elastic energy in the test arrangement. The testing machine has often relatively high stiffness that limits the elastic energy. But the uniaxial tensile test specimen has a large area that contains elastic energy, while this specimen geometry is made to limit the area that is deformed. Thus, the uniaxial tensile test is preferred to determine the stress-strain curve until necking, while this test specimen seems able to evaluate strain hardening at higher strains. However, the drawback is often limited accuracy when measuring the small displacements, and tests with many parallels are required to evaluate the experimental uncertainties.

2.2 Parallel tests to evaluate experimental uncertainties

Additional tests were run with samples from a rectangular extruded cross section with width 200 mm and thickness 3 mm. Herein the test samples were oriented 0º, 45º and 90º relative to the extrusion direction, both shear and tensile loading were investigated, and these tests were run with ten parallels as illustrated in figure 7. Some experimental scatter was observed in the first part up to about 50 MPa, while the initial stiffness above this shows acceptable variation. It seems like the specimen tolerances ± 0.02 mm, that result in a gap in the range 0 – 0.04 mm around the specimen, may not significantly influence the test result. Moreover, the fixation offered by a careful torque applied to the two cylinder head bolts at each specimen end seems to work as expected to prevent lateral torsional buckling of the test specimen. Therefore, it is likely that most of the variation seems related to variation in material properties.

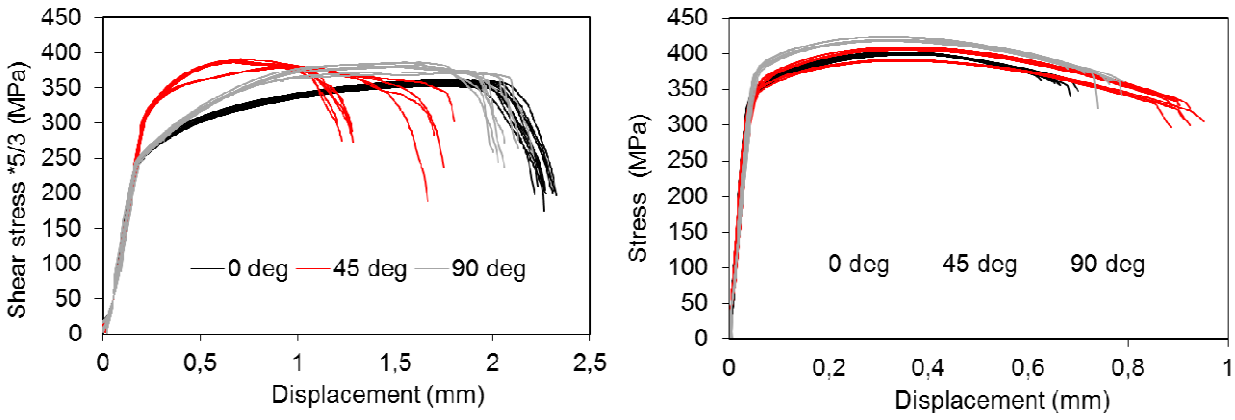

Fig. 7: Results from specimens oriented 0º, 45º and 90º that are tested under shear or stretching

The effect of anisotropy is prominent. The test samples oriented 45º show the lowest ductility under shear loading, while they have the highest ductility under stretching. Moreover, The 90º curves are somewhat above the 0º curves, and all samples under stretch loading shows similar shaped response curves. This indicates that the strain hardening at strains beyond necking can be found by inverse modelling of this specimen under stretching.

The last part of the curves shows some variation, and this variation is more prominent when the specimen is under shear loading than under stretching. Herein, especially the test samples oriented 45º shows higher strength in the first part, more scatter, and reduced ductility compared with the 0º and 90º samples under shear loading. Achani [2] has investigated nearly the same material by using the shear specimen with outer dimensions 80x150 mm, and it seems like the simple test specimen and a holder that fits inside out testing machine gives the same main results as he found, see figure 2.

3 Numerical simulations to evaluate the local variation in material properties

The shear testing arrangement was modelled with LS-DYNA. Both specimen and holder were represented with solid elements, the gap was included, and realistic clamping was modelled with artificial temperature to pretension the bolts, see figure 8. The simulations confirm that the initial variation caused by varying gap between the parts is acceptable as long as the specimen tolerance is within ± 0.02 mm. Herein, this can be seen in figure 9 as the deviation from a straight line in the first part of the response curve up to about 50 MPa.

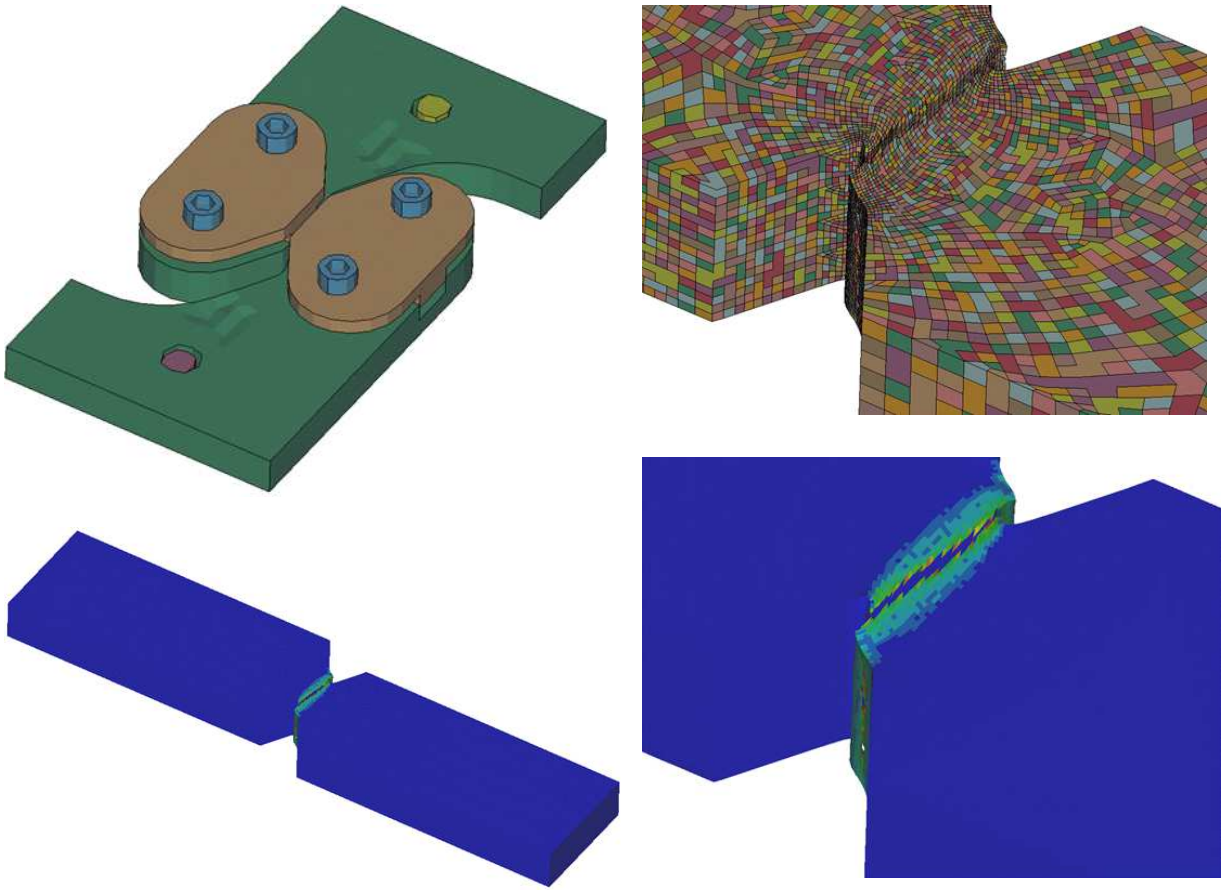

Fig. 8: Numerical model of the shear test arrangement and test specimen with predicted deformation

However, the main effect illustrated in figure 9 is how the predicted deformation mode as well as the last part of the response curve depends on the local variation in material properties. Herein, this was investigated by defining several material definitions with somewhat different ductility randomly spread

among the solid elements that make the test specimen geometry. The result is shown as a more rounded last part of the response curve, and this has an interesting parallel to different fracture models where the damage evolution can be defined by a curve that starts carefully at a certain level of strain and accelerates towards failure. But in this case the material definition is simple whereas the elements handle the deformation mode when some elements are deleted to represent a pore that develops. It is likely that also the yield stress and the strain hardening have local variations that can be handled similarly. It is also interesting to notice that local material variations within 0.1 – 0.2 mm seems to influence the deformation mode when the specimen is under shear, while the same specimen under stretching shows less variation as a result of a larger region that is critical.

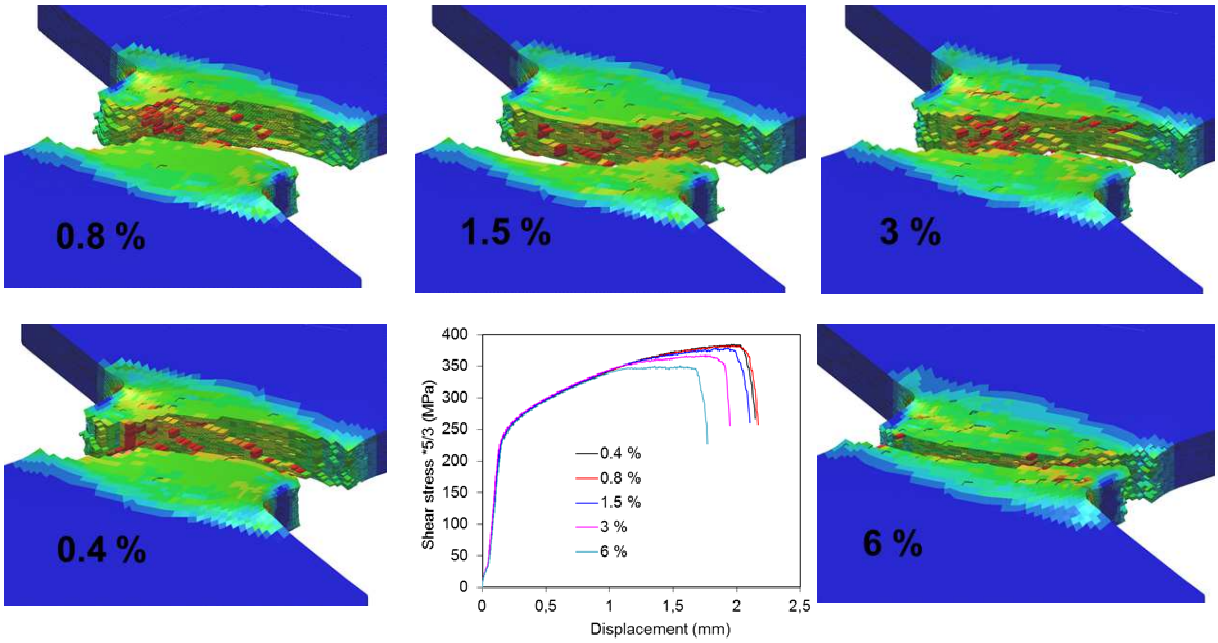

Fig. 9: Simulation results that show the effect of the fraction that has the lowest ductility

Figure 10 illustrates the anisotropic yield criterion formulated by Aretz et al. [4, 5] and calibrated with data from Achani et al. [2, 6].

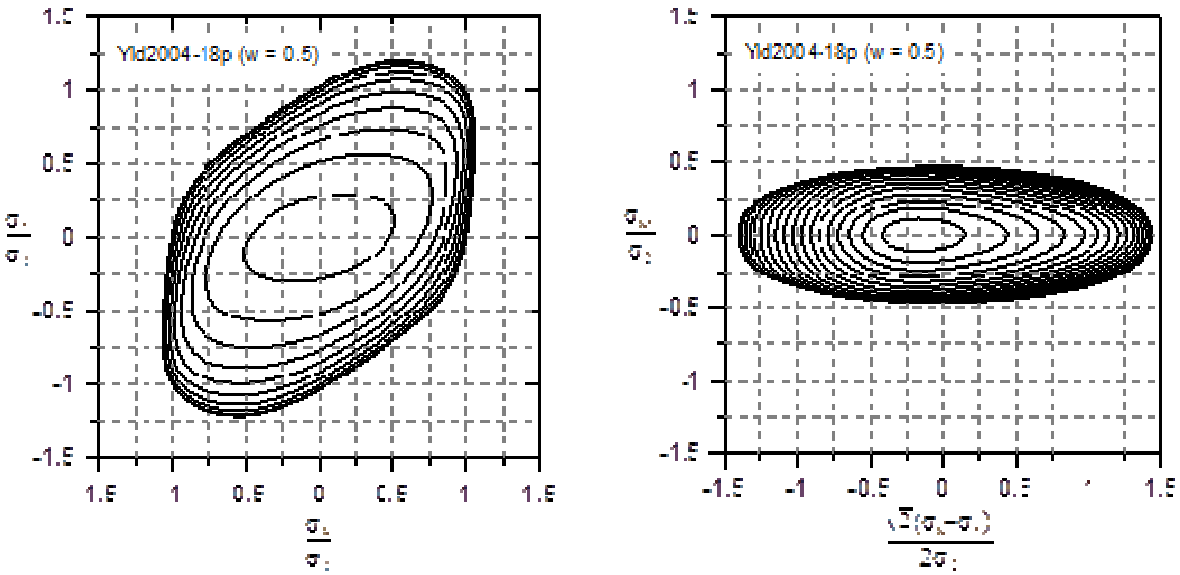

Fig. 10: Yield surface from Achani et al. [2, 6]

3.1 Numerical simulations to evaluate the effect of element size

The coarse variant of specimen geometry had 1 mm solids and an outer skin of shells to capture the surface strain. The intermediate mesh had 0.25 mm solid elements, while the fine variant had 0.1 mm solids. The local variation in material properties was introduced to all of them as somewhat different stress-strain curves as well as somewhat different values for the Cockcroft-Latham parameter that were randomly spread among the elements that define the specimen geometry. The results shown in figure 11 illustrates that the mesh with 1 mm solids are too coarse to be able to capture the localised shear band that is observed in the test. But 0.25 mm solids seems sufficient for the practical engineer, and it is interesting to notice that this mesh in combination with the anisotropic yield surface and the Cockcroft-Latham parameter also predicts the reduced ductility that was observed for the specimens taken at 45º relative to the extrusion direction.

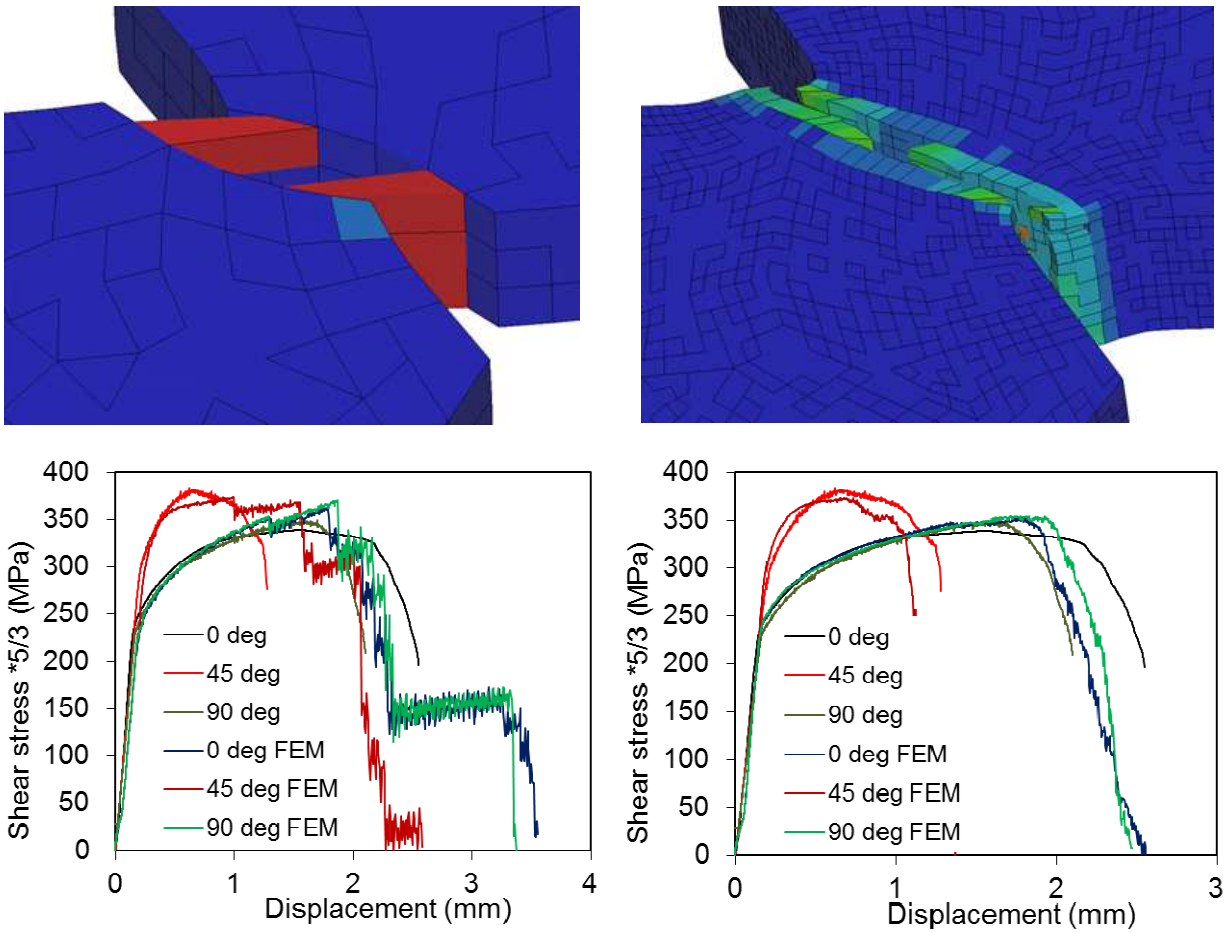

Fig. 11: Predicted deformation mode for 0º, and response curves with 1 mm and 0.25 mm solids

3.2 The practical engineer has to balance the cost for the elements and the material model

It is often not possible to use a mesh where the elements are able to predict the correct deformation mode. The overall deformation mode may look acceptable, but deviations are found when looking into the details. Herein, the deformable barriers made of honeycomb blocks may illustrate how the practical engineer has to find the balance between elements and material model. One option could be sufficient scaling with shell elements to represent local and global folding of the honeycomb structure and a simple material model [7]. The alternative may be a coarse solid model to represent the geometry and a complicated material model to represent the anisotropic behaviour. This balance is not straight forward, and the enormous computational cost between close to cubic shaped solids to avoid looking effects and shell elements with size above the thickness makes it not easier. But also a

complicated material model may require a lot of computational resources, and it may be difficult to calibrate.
The test specimen used in this study is relatively small compared with the thickness, and it can be easily represented with several solid elements through the thickness. Also somewhat larger components like the three chamber profile used in a simple crushing test can be represented by solid elements as shown in figure 12. Herein, the anisotropic yield criteria Yld2004-18p [4, 5] results in a folding modes that are slightly more localised, and there seems to be somewhat more cracks. However, the computational time increases by a factor of four, and it could be interesting to use this on a refined mesh instead. Three solid elements through the thickness is not sufficient for the test specimen in figure 11, and this may be the case also for crushing of the three chamber profile.

The local variation in material properties is introduced randomly from one 0.7 mm solid elements to its neighbours, and this results in crack development at the locations where a severe deformation mode correspond with locally reduced ductility.

Figure 12 also include the results from a simulation with 5 mm shell elements which means 7 – 14 elements over the width of each wall that build up the profile cross section. The wall thicknesses are 1.5 mm, 2.5 mm and 3.5 mm respectively, the width-to-thickness ratio vary from 10 to 45 and the predicted force level seem to be about 18 % too low.

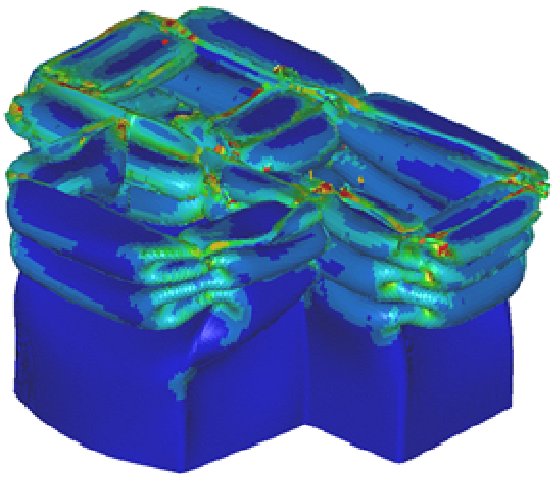

0.7 mm solids + Yld2004-18p

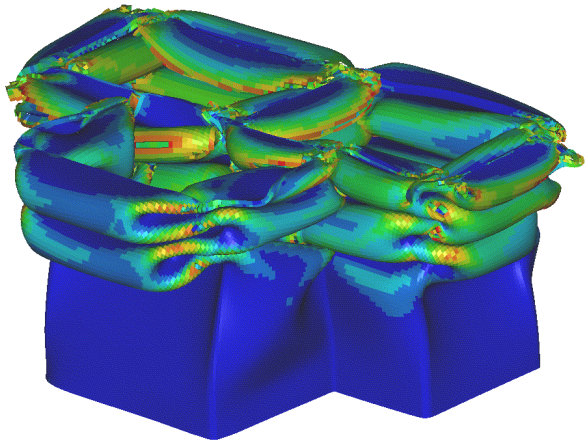

0.7 mm solids + MAT_107

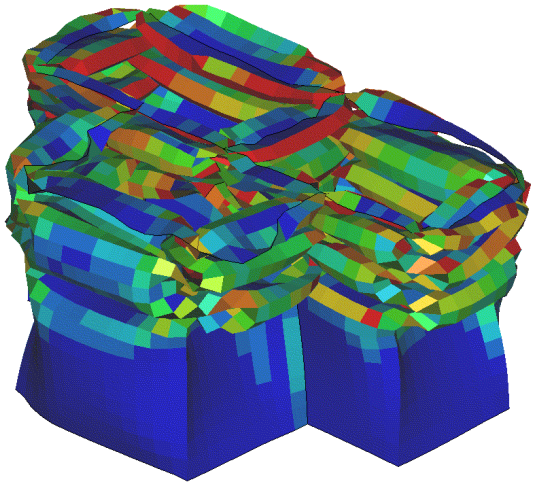

5 mm shells + MAT_107

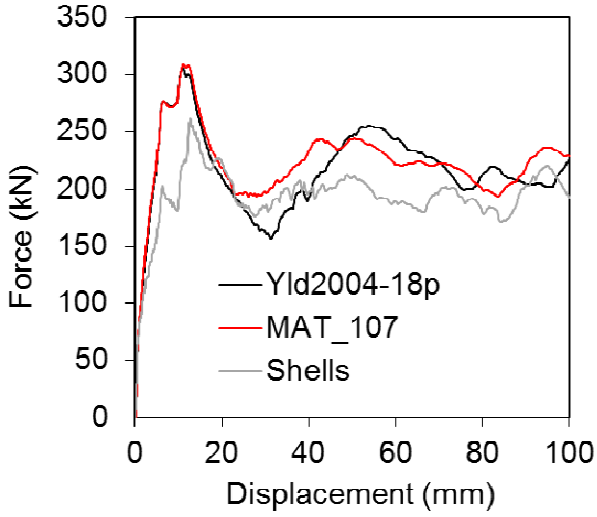

Fig. 12: Predicted response curves as well as deformation mode with shells, solids and anisotropy

Note that all the simulations shown in figure 12 have the same value for the Cockcroft-Latham parameter, and this value comes from inverse modelling of the two tests with the simple specimen. Herein the specimen under stretching is used to find the strain hardening above necking, while the specimen under shear is used to define the parameter for ductile fracture. Both models with 0.7 mm solid elements and the model with 5 mm shell elements seems able to find the chamber with wall thickness 3.5 mm, the connections between the thickest and the thinnest walls as well as the first fold in one of the two corners with wall thickness 2.5 mm as the locations that develop the most severe cracks.

It is likely that some regularisation is required when using larger elements in large scale analysis, but this can be evaluated by using the same element size and element formulation for inverse modelling of the specimen under shear and stretch loading.

4 Summary

It seems like the material ductility as well as the local variation in material properties can be evaluated by use of this simple test specimen and a holder that allows automatic mounting of extensometer. Herein, inverse modelling is important to determine the strain hardening at large strains which means all the way until fracture.

5 Literature

[1] Tryland, T.; "A Simple Compression Test to Evaluate Ductility", 9th Nordic LS-DYNA Users Forum, Göteborg, Sweden, 2008.

[2] Achani, D.: "Constitutive models of elastoplastictiy and fracture for aluminium alloys under path change", PhD thesis, Department of Structural Engineering, NTNU, Trondheim, Norway, 2006, ISBN 82-471-7906-2, page 133-135.

[3] Tarigopula, V., Hopperstad, O.S., Langseth, M., Clausen, A.H., Hild, F., Lademo, O-G., Eriksson, E.: "A study of large plastic deformations in dual phase steel using digital image correlation and FE analysis", Experimental Mechanics 2008, 48(2), page 181-197.

[4] Aretz, H.: "A non-quadratic plane stress yield function for orthotropic sheet metals", J. Mater. Process Technol. 2004, 168, page 1-9.

[5] Barlat, F., Aretz, H., Yoon, J.W., Karabin, M.E., Brem, J.C., Dick, R.E.: "Linear transformation based anisotropic yield functions", Int. J Plasticity 2005, 21, page 1009-1039.

[6] Achani, D., Lademo, O-G., Engler, O., Hopperstad, O.S.: "Evaluation of constitutive models for textured aluminium alloys using in-plane tension and shear tests", Int. J Mater Form 2011, 4, page 227-241.

[7] Tryland, T.; "Alternative Model of the Offset Deformable Barrier", 4th LS-DYNA Users Forum, Bamberg, Germany, 2005.